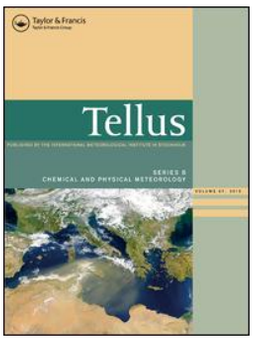

Tellus B: Chemical and Physical Meteorology

ISSN: (Print) 1600-0889 (Online) Journal homepage: http://www.tandfonline.com/loi/zelb20

Size-segregated chemical, gravimetric and number distribution-derived mass closure of the aerosol in Sagres, Portugal during ACE-2

C. Neusüß, D. Weise, W. Birmili, H. Wex, A. Wiedensohler & D. S. Covert

To cite this article: C. Neusüß, D. Weise, W. Birmili, H. Wex, A. Wiedensohler & D. S. Covert (2000) Size-segregated chemical, gravimetric and number distribution-derived mass closure of the aerosol in Sagres, Portugal during ACE-2, Tellus B: Chemical and Physical Meteorology, 52:2, 169-184, DOI: 10.3402/tellusb.v52i2.16091

To link to this article: https://doi.org/10.3402/tellusb.v52i2.16091

Published online: 15 Dec 2016.

Tellus (2000), 52B, 169–184
Printed in UK. All rights reserved

TELLUS
ISSN 0280–6509

Size-segregated chemical, gravimetric and number distribution-derived mass closure of the aerosol in Sagres, Portugal during ACE-2

By C. NEUSÜß[1]*, D. WEISE[1], W. BIRMILI[1], H. WEX[1], A. WIEDENSOHLER[1] and D. S. COVERT[2],
[1]*Institute for Tropospheric Research, Permoserstrasse, 15, D-04318 Leipzig, Germany;* [2]*Department of Atmospheric Sciences, University of Washington, Box 354235, Seattle, WA 98195-4235, USA*

(Manuscript received 8 February 1999; in final form 17 September 1999)

ABSTRACT

During the ACE-2 field campaign in the summer of 1997 an intensive, ground-based physical and chemical characterisation of the clean marine and continentally polluted aerosol was performed at Sagres, Portugal. Number size distributions of the dry aerosol in the size range 3–10 000 nm were continuously measured using DMPS and APS systems. Impactor samples were regularly taken at 60% relative humidity (RH) to obtain mass size distributions by weighing the impactor foils, and to derive a chemical mass balance by ion and carbon analysis. Hygroscopic growth factors of the metastable aerosol at 60% RH were determined to estimate the number size distribution at a relative humidity of 60%. A size segregated 3-way mass closure study was performed in this investigation for the first time. Mass size distributions at 60% RH derived from number size distribution measurements and impactors samples (weighing and chemical analysis) are compared. A good agreement was found for the comparison of total gravimetrically-determined mass with both number distribution-derived (slope = 1.23/1.09; $R^2 > 0.97$; depending on the parameters humidity growth and density) and chemical mass concentration (slope = 1.02; $R^2 = 0.79$) for particles smaller than 3 μm in diameter. Except for the smallest impactor size range relatively good correlations (slope = 0.86–1.42) with small deviations ($R^2 = 0.76$–0.98) for the different size fractions were found. Since uncertainties in each of the 3 methods are about 20% the observed differences in the size-segregated mass fractions can be explained by the measurement uncertainties. However, the number distribution-derived mass is mostly higher than the chemically and gravimetrically determined mass, which can be explained by sampling losses of the impactor, but as well with measurement uncertainties as, e.g., the sizing of the DMPS/APS.

1. Introduction

Anthropogenic aerosols play a significant rôle in global climate by modulating radiation transfer. Aerosol particles can effect the earth's radiative balance directly through the increased scattering and absorption by anthropogenic particles (Charlson et al., 1991). Anthropogenic particles may also influence climate indirectly by modifying the number concentration, composition and size of cloud droplets, and subsequently, cloud albedo (Twomey, 1977). Regional and global models are required to quantify the direct and indirect effects of particles on climate. Aerosol chemical composition and size distribution parameters representative of aerosols under clean and polluted conditions are needed as input variables to models to differentiate between the effect of anthropogenic aerosols and those of the natural aerosol.

* Corresponding author.
e-mail: neusuess@tropos.de

Closure experiments are necessary to validate the input and output parameters used by and derived from models and to identify and estimate associated uncertainties in these parameters (Quinn et al., 1996).

A fundamental and important issue in characterising the atmospheric aerosol is the determination of the aerosol mass concentration as a function of particle size. There are 3 different methods to obtain size-segregated aerosol mass: (a) the gravimetric method (weighing of sampled aerosol), (b) the summation of all analysed chemical compounds and associated water, and (c) the calculation of the particle mass distribution from the number size distribution.

In the past, mass closure studies have had varying success and large uncertainties for single samples and specific size ranges although time and size averages have shown better agreement (Quinn and Coffman, 1998). Sampling and detection techniques are becoming increasingly better with time but for particle sizes ($D_P > 5$ μm) sampling and counting errors are still large. This is especially critical since just a few coarse mode particles can be responsible for a major mass fraction. On the other hand, particles in the 0.1 to 1 μm diameter range are most strongly influenced by anthropogenic emissions and have the largest effect on short-wave radiative transfer.

In this study, we applied in-situ measurements of physical and chemical aerosol parameters taken at Sagres, Portugal during the second Aerosol Characterisation Experiment (ACE-2) (Russell and Heintzenberg, 2000) to perform a size-segregated aerosol mass closure between the 3 different methods mentioned above. A similar and successful mass closure for ACE-1 has been performed for 2 size fractions (Quinn and Coffman, 1998). Here 4 size fractions were investigated. Furthermore, the chemical analysis was extended from the determination of major ions to the analysis of ions and carbon. Since the impactor samples were collected and weighed at a relative humidity of 60%, a concerted effort was made to include hygroscopic growth of aerosol particles to calculate the hydrated particle number and mass distribution.

In this investigation, we present mass closure studies of 15 time periods where impactor samples for mass were compared with the mass balance of the chemical analysis and the mass calculated from number size distributions and hygroscopicity measurements.

2. Measurements

During ACE-2, intensive in-situ measurements were performed at the Sagres-50 site located on a Portuguese Naval Base 1 km north-west of the village of Sagres, about 1 km from the west coast and 100 m from the south coast, and 50 m above sea level at the south-western tip of Portugal (8°57′ W, 36°59′ N).

The nearby surroundings especially to the north are relatively uninhabited and unaffected by human activities. The measurements were minimally influenced by the village Sagres since the main wind direction was from the north-northwest and the Atlantic Ocean. During periods of more northerly winds, the air mass was influence by power plants and other human activities along the west coast of Portugal.

The instrumentation for the in-situ, physical and optical characterisation of the aerosol was housed in an air-conditioned container. The samplers for chemical analysis were housed in a shelter at the base of the sampling stack. A modified high-flow Anderson PM 10 inlet operating at a flow rate of 300 l/min at the top of the stack conditioned the air flow used for impactor and filter sampling for mass and chemical analysis. A low-flow Anderson PM 10 inlet (16.7 l/min) conditioned the air flow used for (among other things) particle number concentration, number size distribution, and hygroscopicity measurements. Both inlets were mounted about 20 m above ground level to avoid near-ground dust and other aerosol sources.

2.1. *Number size distribution*

Number size distributions were measured using a high resolution Twin Differential Mobility Particle Sizer (TDMPS) (Birmili et al., 1999). A TDMPS consists of 2 DMA-based (Differential Mobility Analyser) size spectrometers (DMPS) operating in parallel. One DMPS measures the size distribution between 3–20 nm. The second DMPS covers the range 20–800 nm. The TDMPS system provides an automated flow control of the aerosol inlet flow rates for stable long-term

operation. The size distribution in the larger size range (between 0.8–10 μm) was measured by an Aerodynamic Particle Counter (APS, TSI model 3310). Unfortunately, the upper size range of the APS ($D_p > 3$ μm) was strongly influenced by false counts leading to an overestimate of the number concentration in that range and thus a large error in the mass size distribution. The number distributions of the TDMPS and APS were measured at relative humidities (RH) less than 10%. The APS number distribution was converted from aerodynamic diameter to Stokes diameter (geometric in case of spherical particles) with an assumed density of 2 g/cm^3 since according to chemical analyses the main chemical component was sea-salt (Tang and Munkelwitz, 1994).

2.2. Mass-size distribution

Two 6-stage Berner impactors (Berner and Lürzer, 1980) with 50%-size cuts at 0.05, 0.14, 0.42, 1.2, 3.5, and 10 μm aerodynamic diameter (D_{ae}) were used for aerosol sampling. The sampling time varied between 6 and 36 h but was typically around 12 h. The RH in the impactor was controlled in order to (i) maintain size cuts independent of variation in the ambient RH, e.g., during day–night changes, and (ii) derive aerosol properties comparable to other measurements (HTDMA) and (iii) limit the volume fraction of water. At a RH of 60%, the particles were expected to stick to minimise bounce-off. In previous closure studies (Quinn and Coffman, 1998) a lower humidity was possible, since more hygroscopic particles (in a less anthropogenic region) were abundant. At the bottom of the inlet, 2 bundles of seven 1.5 m by 0.95 cm diameter tubes were used to control the aerosol RH. The RH of the aerosol was measured at the impactor inlet and was controlled by heating the tube bundles. Model results indicate that the temperature of the air at the outlet is in thermal equilibrium with the tube bundle. Thus, the maximum temperature increase was about 10°C. The RH was usually controlled at 60 ± 2%, however, the RH was during daytime sometimes lower, but rarely below 50%.

Tedlar (polyvinylfluoride) and aluminium foils were used as sampling substrates in the impactor for the analysis of particulate mass plus ionic compounds and mass plus organic and elemental carbon, respectively. Prior to sampling, the Tedlar foils were cleaned with deionised water, then with diluted H_2O_2, and finally several times, with pure water again. The aluminium foils were preheated to 350°C for several hours to drive-off volatile compounds.

The mass of the samples was determined by weighing the foils before and after exposure using a Mettler UMT 2 microbalance (Mettler Toledo, Greifensee, Switzerland). The microbalance was placed in a box with a constant RH of approximately 60%. The constant RH was provided by a saturated NaBr solution and was continuously controlled. The foils were conditioned in this box for at least 12 h before weighing.

2.3. Size-segregated chemical analysis

Organic, and elemental carbon were determined by a thermal desorption method using a commercial system (5500 c-mat, Ströhlein, Kaarst, Germany). The sample is placed in a quartz tube and rapidly heated to a specific temperature. To separate organic and elemental carbon the sample is firstly heated under nitrogen to 500°C. Those carbon compounds which evaporate under these conditions are referred to as volatile carbon. In a second step, the sample is heated under oxygen to 650°C, where all carbon except carbonate is oxidised. This carbon mass is referred to non-volatile carbon (Petzold, 1995). In both cases, the evaporated carbon is completely oxidised to CO_2 ($T = 850$°C, CuO-catalysator), which is subsequently analysed using an IR-detector. Calibration is performed by running external standards. All values are corrected for field blanks.

The exposed Tedlar foils were cut into small pieces, leached in 1 ml of deionised water (18 MΩ/cm, Nanopure Wilhelm Werner GmbH), which was then filtered and analysed by capillary zone electrophoresis. A Spectra Phoresis 1000-instrument from Thermo Separation Products (now Thermoquest, San Jose, California) equipped with a fused silica capillary with an inner diameter of 75 μm and a total length of 70 cm (63 cm to the detector) was used. The applied electrical field was 420 V/cm. The buffer used to determine anions consists of an aqueous solution of p-aminobenzoate (10 mmol/l), NaOH (resulting in a pH of 9.6), and 8 mmol/l diethylenetriamine. Indirect detection is performed with a diode array detector operating at $\lambda = 254$ nm (Röder and

Bächmann, 1995). The buffer to separate the main inorganic cations contains Imidazol (5.5 mmol/l), phosphoric acid (5 mmol/l) and 18-crone-6 ether (2.5 mmol/l, to separate ammonium and potassium (Beck and Engelhardt, 1992; Yang et al., 1994)).

For every sample, a blank value was determined by analysing a part of the foil without sample deposit. Blank values for stages 2 to 5 never reached levels significant compared to the chemical mass of the corresponding samples, i.e., less than 1%. For stage 1 the blank values accounted for less than 10% of the chemical mass.

2.4. *Hygroscopicity*

A Hygroscopic Tandem Differential Mobility Analyser (HTDMA, Swietlicki et al., 2000) was used to measure in-situ, size-segregated hygroscopic growth factors of aerosol particles in the size range 35–250 nm in diameter. In the HTDMA, a growth factor, i.e., a change in diameter is determined when aerosol particles are taken from a low relative humidity (< 10% RH) to a hydrated state at a controlled higher RH. The HTDMA consists of 3 main parts:

(1) DMA-1 which selects a narrow quasi-monodisperse aerosol from the entire atmospheric aerosol population at low RH,
(2) humidifiers which condition the sheath air of DMA-2 and the monodisperse aerosol from DMA-1 to an RH of 60% or 90% RH in this experiment and
(3) DMA-2 which measures the distribution of particle growth caused by the imposed humidification.

During standard operation conditions, the humidity in DMA-2 was kept at 90% RH but it was changed to 60% RH about once a day to correspond to the RH at which the impactor samples were collected and weighed. The particle growth at 60% RH was measured for increasing as well as for decreasing RH (from 10% and 80%, respectively) to determine the effect of hysteresis on particle hydration. A small but significant hysteresis effect could be measured. Growth factors determined for decreasing RH have been used for calculation of water content of the impactor samples since this condition is most likely for the particles as they existed in and were sampled from the atmosphere.

3. Calculations and error discussion

3.1. *Number-derived mass distribution*

To enable closure experiments between the impactor-derived mass-size distributions (at 60% RH) and the TDMPS and APS number distribution measurements, the measured distributions were converted to a common RH and common size increments.

(1) First, the number-size distributions were averaged over the time period of the impactor samples.
(2) The number distributions (RH < 10%) were converted to number distributions at 60% RH. Measured HDTMA growth factors were used for the sulphate dominated submicrometer size range, and values from Tang et al. (1997) were used for the sea-salt dominated supermicrometer size range.
(3) From this number distribution at 60% RH, the mass distribution was calculated assuming densities of 1.35 and 1.4 g/cm^3 (Table 1). This estimation is based on the chemical composition and volume fraction of water at RH = 60% (NaCl: 1.29, $NaNO_3$: 1.54, Na_2SO_4: 1.72, $(NH_4)_2SO_4$: 1.35, $(NH_4)_3H(SO_4)_2$: 1.38, NH_4SO_4: 1.39 (g/cm^3); Tang and Munkelwitz, 1994).
(4) The same densities were used to recalculate the impactor-derived mass size distribution from aerodynamic to Stokes diameter.
(5) For quantitative comparison, the mass size distribution calculated from the DMPS/APS was integrated over the size intervals corresponding to the impactor cut-offs.

The measurement uncertainties of the TDMPS, APS, and HTDMA systems are mainly due to concentration and sizing errors, resulting from deviation of the flows from their nominal values. Furthermore the particle density has to be estimated. The aerosol concentration and sizing accuracy of the TDMPS might be up to 10% and 5%, respectively. The sizing error includes measurement uncertainties, but moreover, includes the shape factor of the particles which can be different from one. Sensitivity studies for a typical continental aerosol show a difference in mass

Table 1. *Overview over impactor characteristics and parameters for 2 scenarios of calculating mass size distributions from number size distributions*

Stage no.	Aerodynamic particle diameter (50% cut-off of impactor) (μm)	Corresponding Stokes diameter (density 1.4 g/cm^3) (μm)	Scenario 1		Scenario 2	
			Hygroscopic growth factor	Density @ (60% RH) (g/cm^3)	Hygroscopic growth factor	Density @ (60% RH) (g/cm^3)
1	0.05–0.14	0.042–0.118	1.18	1.4	1.1	1.35
2	0.14–0.42	0.118–0.355	1.18	1.4	1.1	1.35
3	0.42–1.2	0.355–1.014	1.2	1.4	1.15	1.35/1.4*
4	1.2–3.5	1.014–2.959	1.25	1.4	1.25	1.4
5	3.5–10	2.959–8.452	1.25	1.4	1.25	1.4

* Densities for calculating Stokes diameters at both cut-offs of the impactor stage.

concentration of 15% for a sizing uncertainty of 5%. The density correction of the dry aerodynamic number-size distribution measured with the APS to Stokes diameter may contain a systematic error of 5–10%. Errors due to counting statistics are low, since the number size distribution measurements are averaged over the impactor collection time of 6–36 h. The precision of growth factors determined by the HTDMA is about 3%. The overall uncertainty of the number-derived mass concentration results are thus about $\pm 20\%$. Since the growth of the particles to 60% RH has been determined only occasionally the variation over time has not been considered.

3.2. *Gravimetrically-derived mass distribution*

Both the chemical and the gravimetric analyses are based on the samples collected with the impactor. The flow uncertainty was not determined but is expected to be constant since a critical orifice was used and the vacuum continuously measured. The mass concentrations have a linear response to flow uncertainties. Errors in the size cuts lead to a different distribution but minimally influence the total mass concentration. The same statement is valid for the sharpness of the size cuts and in part for bounce and shatter of particles. Few studies have been done on the performance of Berner impactors (Reineking et al., 1984; Wang and John, 1988; Hillamo and Kaupinen, 1991; Howell et al., 1998). None of these studies were done for the particulate type of Berner impactor used in this study. Nevertheless, these studies are a good measure of the sampling characteristics. Wang and John found sharp size cuts with a difference of 4.5% and 18% for the 50% cut-off compared to the values of the manufacturer for the super- and submicrometer particles, respectively. Hygroscopic growth due to jet expansion can be neglected for a RH smaller than 70%. Bounce-off is small for greased substrates as well as for ammonium sulphate (at RH 60% about 10% loss). Losses of ammonium nitrate are much smaller than when sampled with a filter. This fact seems to be of lesser interest for this experiment since all nitrate was found (as non-volatile salts) in the coarse mode (Table 2) but might be interesting in terms of giving an argument for complete sampling of other semivolatile species like organics. Howell et al. (1998) found good agreement in the mean diameter of ionic species for Berner and MOUDI impactors, although single differences were partly high and large particles were badly collected due to inlet losses. We used a modified Sierra high volume sampler inlet for which inlet losses are demonstrated in the same paper to be less important.

In summary, there are some sampling losses in the impactor, though difficult to quantify, are probably about 10%. Independent of these systematic errors a statistical uncertainty for gravimetric mass distribution can be derived from mass determinations of the 2 parallel sampled impactors. The difference in mass between the 2 impactors (sampling and weighing uncertainties) was between 8 and 13% for impactor stages 2 to 5 and about 40% for impactor stage 1. Field blanks were taken, but no systematic change in mass was observed. Thus, quantifiable uncertainties of the

Table 2. *Overview over relevant data for all 15 presented cases (all values in μg/m³)*

Sample														DMPS/APS	
begin	end	Particle size	NH_4^+	K^+	Ca^{2+}	Na^+	Mg^{2+}	Cl^-	NO_3^-	SO_4^{2-}	N_2O	Chem. mass	Grav. mass	Scen. 1	Scen. 2
178.31	178.57	stage 1	0.02	0.00	0.00	0.01	0.00	0.00	0.00	0.03	0.02	0.08	0.00	0.16	0.15
		stage 2	0.17	0.00	0.00	0.02	0.00	0.00	0.00	0.26	0.18	0.69	0.34	1.04	0.85
GD 5		stage 3	0.02	0.01	0.01	0.26	0.02	0.22	0.08	0.13	0.27	1.06	0.58	0.93	0.75
		stage 4	0.01	0.05	0.03	1.31	0.10	1.46	0.20	0.21	5.08	8.49	4.01	4.32	4.13
clean		stage 5	0.01	0.04	0.04	0.91	0.09	1.25	0.03	0.17	4.01	6.55	2.77		
		sum 1–4	0.21	0.06	0.04	1.60	0.12	1.68	0.28	0.64	5.55	10.31	4.93	6.46	5.89
178.59	178.82	stage 1	0.02	0.01	0.00	0.01	0.00	0.01	0.00	0.04	0.03	0.13	0.00	0.11	0.11
		stage 2	0.11	0.00	0.00	0.02	0.00	0.00	0.00	0.37	0.19	0.72	0.00	1.08	0.89
GD 5		stage 3	0.02	0.01	0.01	0.23	0.03	0.24	0.07	0.20	0.30	1.13	0.00	0.98	0.79
		stage 4	0.01	0.03	0.04	1.01	0.11	1.70	0.27	0.26	5.10	8.55	4.78	4.22	4.04
clean		stage 5	0.01	0.03	0.03	0.63	0.07	1.08	0.03	0.15	3.21	5.24	3.18		
		sum 1–4	0.16	0.05	0.05	1.27	0.14	1.95	0.34	0.87	5.62	10.53	4.78	6.39	5.83
178.85	180.33	stage 1	0.02	0.00	0.00	0.00	0.00	0.00	0.00	0.04	0.04	0.15	0.17	0.18	0.17
		stage 2	0.09	0.00	0.00	0.00	0.00	0.00	0.00	0.23	0.15	0.56	0.64	1.05	0.87
GD 5		stage 3	0.01	0.00	0.00	0.12	0.01	0.06	0.05	0.16	0.19	0.75	0.71	1.04	0.83
		stage 4	0.01	0.02	0.03	0.84	0.10	1.29	0.34	0.22	4.03	6.95	3.87	6.10	5.85
clean		stage 5	0.01	0.01	0.02	0.53	0.05	0.93	0.07	0.13	2.73	4.59	3.37		
		sum 1–4	0.13	0.03	0.03	0.97	0.11	1.35	0.39	0.66	4.40	8.41	5.40	8.36	7.72
180.82	181.35	stage 1	0.05	0.00	0.00	0.00	0.00	0.00	0.00	0.13	0.07	0.28	0.38	0.58	0.54
		stage 2	0.20	0.00	0.00	0.00	0.00	0.00	0.00	0.56	0.29	1.10	1.22	1.78	1.40
GD 6		stage 3	0.06	0.01	0.01	0.05	0.01	0.00	0.02	0.25	0.16	0.61	0.66	0.92	0.72
		stage 4	0.00	0.01	0.02	0.35	0.04	0.19	0.64	0.15	1.18	2.65	2.56	4.21	4.05
clean		stage 5	0.00	0.01	0.02	0.27	0.03	0.26	0.35	0.08	1.07	2.11	2.59		
		sum 1–4	0.32	0.02	0.03	0.41	0.05	0.19	0.66	1.10	1.70	4.64	4.83	7.50	6.71
188.35	188.69	stage 1	0.04	0.00	0.00	0.01	0.00	0.00	0.00	0.28	0.14	0.52	0.34	0.80	0.86
		stage 2	0.30	0.00	0.01	0.03	0.00	0.00	0.00	2.05	0.96	3.69	3.74	7.67	7.00
GD 8		stage 3	0.71	0.03	0.03	0.31	0.04	0.00	0.00	6.01	2.67	10.28	11.64	10.50	8.04
		stage 4	0.02	0.06	0.09	1.64	0.17	0.88	1.85	1.04	5.09	11.47	9.31	11.79	11.25
polluted		stage 5	0.01	0.04	0.05	0.93	0.09	0.76	1.06	0.35	3.33	6.81	7.67		
		sum 1–4	1.07	0.09	0.13	1.99	0.21	0.88	1.85	9.38	8.86	25.97	25.03	30.76	27.14
188.73	189.36	stage 1	0.07	0.02	0.00	0.01	0.00	0.00	0.00	0.18	0.12	0.46	0.24	0.50	0.52
		stage 2	0.83	0.05	0.00	0.02	0.00	0.00	0.00	3.13	1.53	5.89	4.05	6.39	5.94
GD 8		stage 3	1.72	0.04	0.02	0.32	0.04	0.00	0.00	6.03	3.00	11.53	10.50	11.03	8.64
		stage 4	0.02	0.06	0.05	1.64	0.17	1.48	1.26	0.81	6.03	12.14	8.40	14.30	13.67
polluted		stage 5	0.01	0.03	0.02	0.98	0.08	1.19	0.74	0.32	4.14	7.69	6.92		
		sum 1–4	2.64	0.16	0.07	1.98	0.21	1.49	1.26	10.15	10.68	30.01	23.19	32.22	28.77
189.94	190.30	stage 1	0.08	0.01	0.01	0.02	0.00	0.02	0.00	0.24	0.15	0.57	0.00	0.49	0.54
		stage 2	0.85	0.02	0.01	0.04	0.00	0.00	0.00	4.09	1.90	7.32	6.84	8.05	7.32
GD 9		stage 3	0.85	0.02	0.02	0.12	0.02	0.00	0.00	5.59	2.56	9.83	15.62	21.54	17.65
		stage 4	0.00	0.04	0.04	1.04	0.11	0.41	1.07	1.33	3.20	7.62	7.11	12.44	11.94
polluted		stage 5	0.01	0.02	0.02	0.47	0.05	0.42	0.54	0.20	1.79	3.73	3.60		
		sum 1–4	1.78	0.09	0.08	1.22	0.13	0.42	1.07	11.24	7.81	25.35	29.57	42.51	37.46
190.41	190.92	stage 1	0.11	0.01	0.00	0.02	0.00	0.01	0.00	0.30	0.17	0.66	0.18	0.67	0.69
		stage 2	1.20	0.02	0.01	0.02	0.00	0.00	0.00	3.91	2.01	7.71	7.39	10.17	9.18
GD 10		stage 3	1.78	0.04	0.02	0.19	0.02	0.00	0.00	5.80	2.98	11.46	15.72	14.71	11.56
		stage 4	0.04	0.04	0.08	1.15	0.13	0.59	1.24	0.82	3.53	7.93	6.69	12.17	11.71
polluted		stage 5	0.01	0.03	0.06	0.73	0.10	0.59	0.79	0.22	2.59	5.28	6.45		
		sum 1–4	3.12	0.10	0.11	1.38	0.16	0.60	1.24	10.82	8.69	27.77	29.97	37.72	33.14
191.35	191.86	stage 1	0.07	0.00	0.00	0.01	0.00	0.00	0.00	0.17	0.14	0.52	0.22	0.63	0.60
		stage 2	0.47	0.00	0.00	0.01	0.00	0.00	0.00	1.43	0.79	3.04	1.90	3.53	3.07
		stage 3	0.49	0.01	0.01	0.13	0.02	0.00	0.00	1.58	0.88	3.37	2.76	3.17	2.40
slightly		stage 4	0.02	0.02	0.03	0.84	0.08	0.88	1.26	0.38	3.59	7.35	4.60	6.86	6.58
polluted		stage 5	0.01	0.02	0.03	0.56	0.06	0.87	0.66	0.20	2.86	5.38			
		sum 1–4	1.04	0.04	0.04	0.99	0.10	0.88	1.26	3.57	5.40	14.28	9.48	14.20	12.65

Table 2 (cont'd)

Sample														DMPS/APS	
begin	end	Particle size	NH_4^+	K^+	Ca^{2+}	Na^+	Mg^{2+}	Cl^-	NO_3^-	SO_4^{2-}	N_2O	Chem. mass	Grav. mass	Scen. 1	Scen. 2
192.81	193.77	stage 1	0.05	0.00	0.00	0.00	0.00	0.00	0.00	0.13	0.08	0.31	0.42	0.59	0.57
		stage 2	0.54	0.01	0.00	0.01	0.00	0.00	0.00	1.44	0.78	2.99	2.66	4.32	3.87
		stage 3	0.97	0.02	0.01	0.18	0.02	0.00	0.00	2.81	1.47	5.67	4.76	5.00	3.83
slightly		stage 4	0.01	0.03	0.08	0.99	0.08	0.81	1.13	0.35	3.53	7.17	6.85	8.65	8.28
polluted		stage 5	0.01	0.02	0.08	0.57	0.05	0.64	0.51	0.16	2.33	4.42	5.32		
		sum 1–4	1.58	0.06	0.10	1.18	0.10	0.81	1.13	4.73	5.86	16.14	14.69	18.56	16.54
194.28	194.79	stage 1	0.06	0.00	0.00	0.00	0.00	0.00	0.00	0.19	0.09	0.34	0.39	0.45	0.46
		stage 2	0.61	0.01	0.00	0.02	0.00	0.00	0.00	2.81	1.23	4.72	4.68	7.37	7.03
GD 11		stage 3	1.47	0.04	0.02	0.48	0.06	0.00	0.00	8.57	3.75	14.42	16.64	16.66	13.28
		stage 4	0.03	0.08	0.12	2.75	0.22	3.84	1.64	1.41	12.69	22.84	15.45	21.73	20.83
polluted		stage 5	0.01	0.03	0.05	1.10	0.11	2.13	0.78	0.47	6.29	11.01	9.42		
		sum 1–4	2.17	0.13	0.15	3.25	0.28	3.84	1.64	12.98	17.75	42.32	37.17	46.22	41.59
198.00	198.35	stage 1	0.24	0.00	0.01	0.01	0.00	0.00	0.00	0.70	0.36	1.39	1.00	2.37	2.44
		stage 2	1.08	0.01	0.01	0.02	0.00	0.00	0.00	3.66	1.86	7.17	7.70	10.13	8.22
GD 12		stage 3	0.94	0.02	0.01	0.30	0.04	0.00	0.00	3.76	1.89	7.28	7.29	8.03	6.20
		stage 4	0.02	0.05	0.01	1.45	0.16	1.34	1.69	0.58	5.58	11.23	12.59	12.51	11.87
polluted		stage 5	0.01	0.03	0.03	0.70	0.07	0.82	0.76	0.22	3.01	5.99	7.27		
		sum 1–4	2.28	0.09	0.04	1.77	0.20	1.34	1.69	8.71	9.70	27.06	28.58	33.04	28.72
199.87	200.37	stage 1	0.22	0.00	0.00	0.01	0.00	0.00	0.00	0.65	0.38	1.46	1.41	1.16	1.17
		stage 2	0.97	0.02	0.01	0.02	0.01	0.00	0.00	3.13	1.73	6.66	7.54	9.73	8.91
		stage 3	1.71	0.06	0.02	0.64	0.09	0.00	0.00	4.54	2.73	10.48	11.17	12.80	9.76
		stage 4	0.03	0.08	0.06	2.29	0.20	1.34	3.41	0.89	7.44	16.26	13.12	15.16	14.42
polluted		stage 5	0.01	0.04	0.06	1.17	0.13	0.90	1.63	0.31	4.17	8.66	9.28		
		sum 1–4	2.93	0.15	0.09	2.96	0.30	1.34	3.41	9.21	12.28	34.86	33.23	38.85	34.26
202.36	202.76	stage 1	0.08	0.00	0.01	0.01	0.00	0.00	0.01	0.21	0.12	0.48	0.56	0.54	0.57
		stage 2	1.16	0.01	0.02	0.02	0.00	0.00	0.00	2.46	1.37	5.27	5.12	8.19	7.59
GD 14		stage 3	1.72	0.03	0.02	0.34	0.04	0.00	0.00	4.39	2.41	9.25	8.02	9.97	7.50
		stage 4	0.01	0.06	0.06	1.65	0.21	1.22	1.63	0.55	5.56	11.09	9.69	10.22	9.81
polluted		stage 5	0.01	0.04	0.07	1.17	0.13	1.15	0.95	0.32	4.45	8.61	9.72		
		sum 1–4	2.97	0.11	0.10	2.02	0.26	1.22	1.64	7.60	9.46	26.10	23.39	28.92	25.47
202.83	203.40	stage 1	0.06	0.00	0.00	0.01	0.00	0.01	0.00	0.15	0.08	0.33	0.46	0.46	0.48
		stage 2	0.79	0.01	0.01	0.02	0.00	0.00	0.00	2.12	1.19	4.57	4.30	7.50	6.78
(GD 15)		stage 3	0.89	0.03	0.01	0.33	0.03	0.03	0.09	2.96	1.62	6.24	6.51	7.87	5.93
		stage 4	0.03	0.06	0.06	1.69	0.17	1.95	1.36	0.55	7.02	13.16	11.38	12.51	12.09
polluted		stage 5	0.02	0.04	0.04	1.21	0.12	1.74	0.73	0.35	5.62	10.05	10.43		
		sum 1–4	1.76	0.10	0.08	2.05	0.21	1.99	1.45	5.78	9.91	24.30	22.65	28.34	25.28

gravimetric mass are about −25% to +5% for stages 2 to 5 and −50% to +30% for stage 1, respectively. Nevertheless, uncertainties of the 50% cut-off diameter and the collection efficiency are not known for this impactor.

3.3. *Chemically-derived mass distribution*

The chemical analysis is both precise and accurate within a few percent as shown by 2 laboratory intercomparisons before and after the field campaign (Putaud et al., 2000). Furthermore, regular intercomparisons with ion chromatography in our laboratory show the accuracy of the complete method used here (i.e., within a few percent). However, the uncertainty is expected to be higher during the field campaign. The ion balance is one measure of the uncertainty of the ion analysis. The ion balance was calculated including H^+ (derived from pH measurements), NH_4^+, K^+, Ca^{2+}, Na^+, Mg^{2+}, Cl^-, NO_3^-, SO_4^{2-}, $C_2O_4^{2-}$, and MSA^-. For 15 cases including stages 2 to 5 the mean of the ion balance is zero, which means that there is no systematic error. The mean of the absolute value of the ion balance is 16%, which should be the magnitude in the uncertainty of the

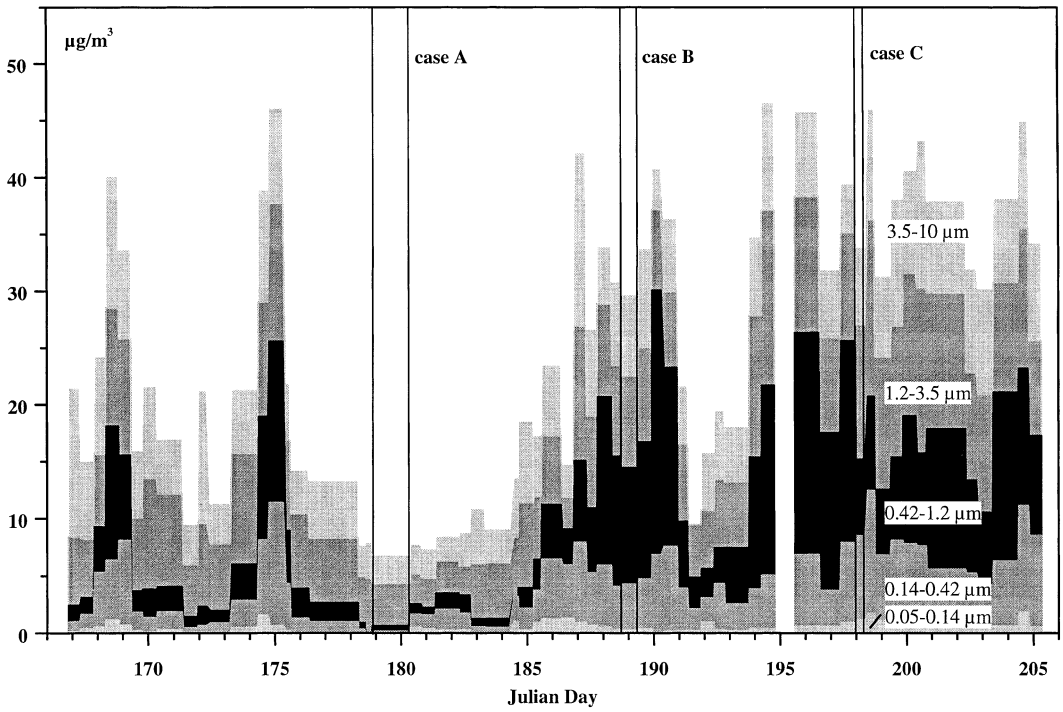

Fig. 1. Mass size distribution for the complete period — 16 June (Julian day 166) to 26 July (Julian day 206) — determined with the impactor (numbers are aerodynamic diameter, relative humidity: 60%).

chemical analysis, independent of the absolute mass loading. Blank values only contribute to the smallest stage (error of 10%, compare Subsection 2.1.3) The overall uncertainties is similar to uncertainties of 20% reported by Quinn et al. (1996).

The uncertainty in the determination of the total carbon (volatile and non-volatile) is estimated to be comparable to the value for the ionic species for polluted air masses, i.e., $\pm 20\%$, mainly caused by variation of blank values. Uncertainties increase for samples with low carbon content (smallest particles, clean air masses) where the carbon content can reach values close to the blank values. Since the total carbon fraction is low for the samples taken in Sagres (mean value 6% of the total mass), uncertainties in its determination does not strongly influence the chemical mass balance. The division between volatile (organic) and non-volatile (elemental) carbon seems to depend strongly on the method used. However, this has no influence on the total carbon amount and only slight influence on the mass of carbonaceous material.

In all, the error of the ionic and carbonaceous mass concentration is estimated to be $\pm 20\%$ ($\pm 30\%$ for stage 1).

The water mass has been calculated based on number derived growth factors (HTDMA) for submicrometer particles and on the ionic composition in the coarse mode. Diameter based growth factors resulting from the HTDMA were converted to volume growth factors, density-corrected and applied to the sum of the chemical mass (ions + carbon = "dry mass"). The main uncertainty in water content is the determination of the growth factor, since it scales as the cube. Here, a growth factor of 1.12 is used. Again, the variation over time has not been considered, since the growth of the particles to 60% RH has been determined only occasionally. For growth factors of 1.06 and 1.25, which are measured values at the upper and lower limit during ACE-2, the water content is about a factor of 2 higher or lower.

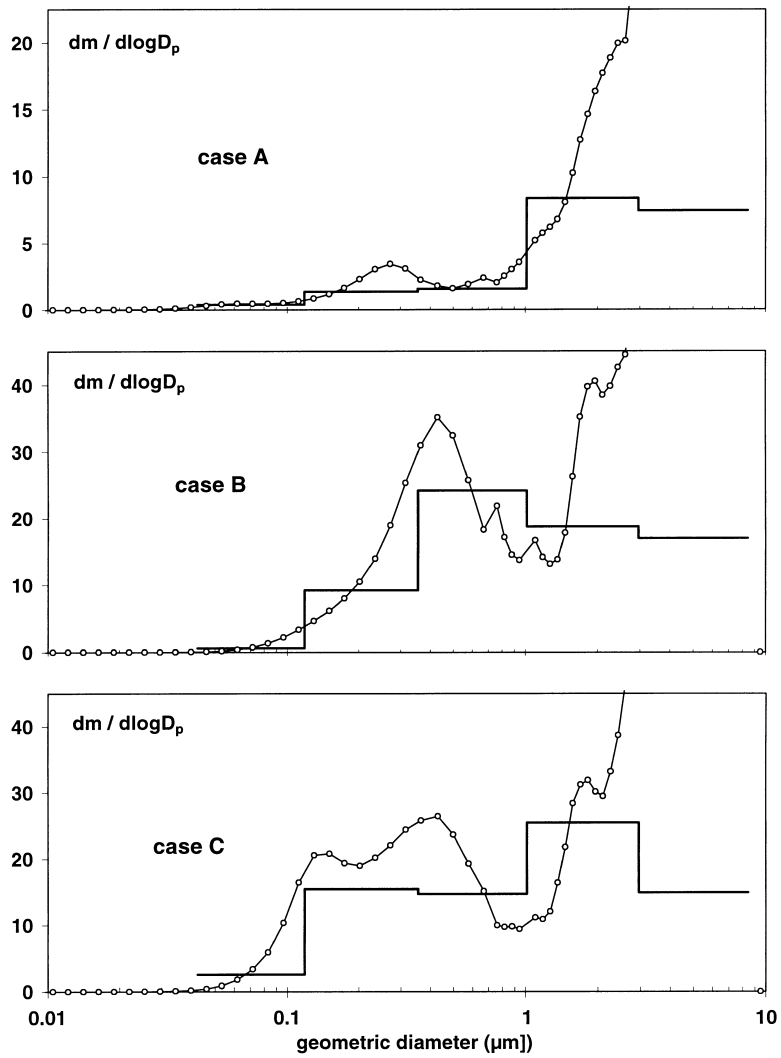

Fig. 2. Mass size distributions at 60% RH from DMPS/APS measurements (dots) and from gravimetric determination (impactor, solid line) for 3 different cases: clean (A), long range transport of pollution (B), and regional pollution (C).

Since the mean water content is about 35% by mass, this leads to a maximum uncertainty for the total chemical mass determination of 18%.

HTDMA-measurements have been performed for particles up to 250 nm in Stokes diameter (in this case for particles of the 2 smallest impactor stages). We used the same values for impactor stage 3 (0.42–1.2 µm) since the chemical composition is only slightly different.

For coarse mode particles data taken from laboratory measurements by Tang et al. (1997) were used to calculate growth factors. The coarse mode consisted mainly of sea-salt where nitrate and sulphate partly replaced the chloride (Fig. 5, Table 2). Assuming only sea-salt (which has the same growth as pure NaCl, Tang et al. 1997), $NaNO_3$, and Na_2SO_4 water amounts were calculated for all impactor measurements based on the measured ratio of chloride to nitrate and sulphate (growth factors are comparable for $NaNO_3$, and

Na_2SO_4 (Tang and Munkelwitz 1994; Tang et al., 1997)). With a density of 1.4 this leads to a mean aerosol growth factor of 1.25.

4. Results and discussion

4.1. Gravimetric versus number derived mass concentration

The mass distributions for the entire sampling period are presented in Fig. 1. The time is given in "Julian day" (0.5 being January 1, noon). A total of 15 samples have been chosen for comparison of impactor and DMPS/APS derived mass size distributions. Most of them were taken from the "Golden days" (Russell and Heintzenberg, 2000), which are characterised by relatively constant conditions with respect to wind direction, backwards trajectories, aerosol absorption, total particle number concentration, and concentration of gaseous species (NO_x, O_3, SO_2). Some additional samples are included to obtain not only examples of polluted (high mass concentration) or clean (low mass concentration) air masses, but also some intermediate mass concentration to make the statistical correlations more robust.

To calculate mass size distributions from DMPS/APS number size distributions, 2 different scenarios have been used. These are summarised along with the impactor characteristics in Table 1. In the first scenario, an aerosol growth factor of 1.18 as a typical value for the first part of the experiment was used. For scenario 2 growth factor of 1.1 was used for the submicrometer range. This value has been measured for more polluted cases during ACE-2. Gravimetric, chemical, and number distribution derived mass concentration for the 15 samples are summarised in Table 2.

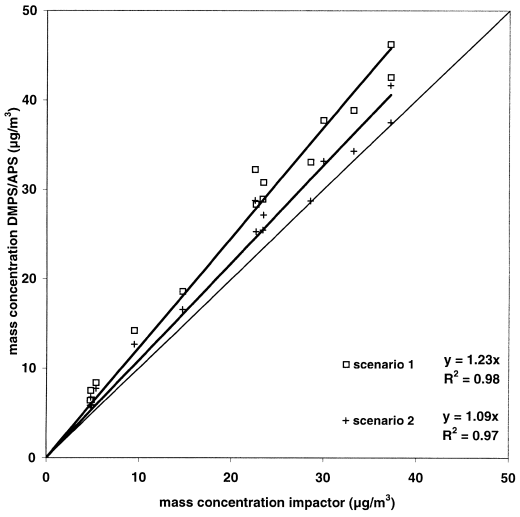

Fig. 3. Comparison of impactor versus DMPS/APS mass concentration for the 2 scenarios (sum over 4 impactor stages, Stokes diameter <3 µm, 60% RH).

Results of the DMPS/APS- and gravimetric mass-size distributions for 3 out of these 15 samples (as marked in Fig. 1) are presented in Fig. 2. The calculations have been performed with scenario 1. Case A represents the clean marine air, trajectories indicating North Atlantic air masses. The mass size distribution has its maximum in the coarse mode range deriving from sea-salt and shows only a small accumulation mode. Case B is an example for long range transport of a polluted air mass from Central Europe over the eastern Atlantic to Sagres. In this case, the mass size distribution shows a significant accumulation and sea-salt mode. Case C represents an air mass that was transported from Central Europe over the Iberian peninsula to Sagres. Here, the mass size distribution is tri-modal with an Aitken mode in addition to the accumulation and sea-salt modes that indicates a polluted but less aged aerosol compared to case B. For particle sizes larger than 3–4 µm, the APS derived aerosol mass seems to increase sharply. But this is due to the counting artefact in the APS. The number concentration greater than 4 µm was constant and significantly larger than zero as a result of false counts which could not be corrected. Thus, the particle size range larger 3.5 µm D_{ae} (impactor stage 5) was excluded. Peaks in the DMPS/APS-derived mass distribution for cases A and B at about 700 nm are probably caused by a mismatch of the DMPS and the APS number distribution. The APS number distribution had to be converted from aerodynamic to Stokes diameter using an assumed particle density of the coarse mode. Since the RH in the APS is not known to better than $\pm 10\%$, the density might have differed from day to day. For the conversion of the APS number size distribution, however, a constant particle density of 2 g/cm^3 was used.

Although the size resolution is limited (5 stages), the different modes determined by the better

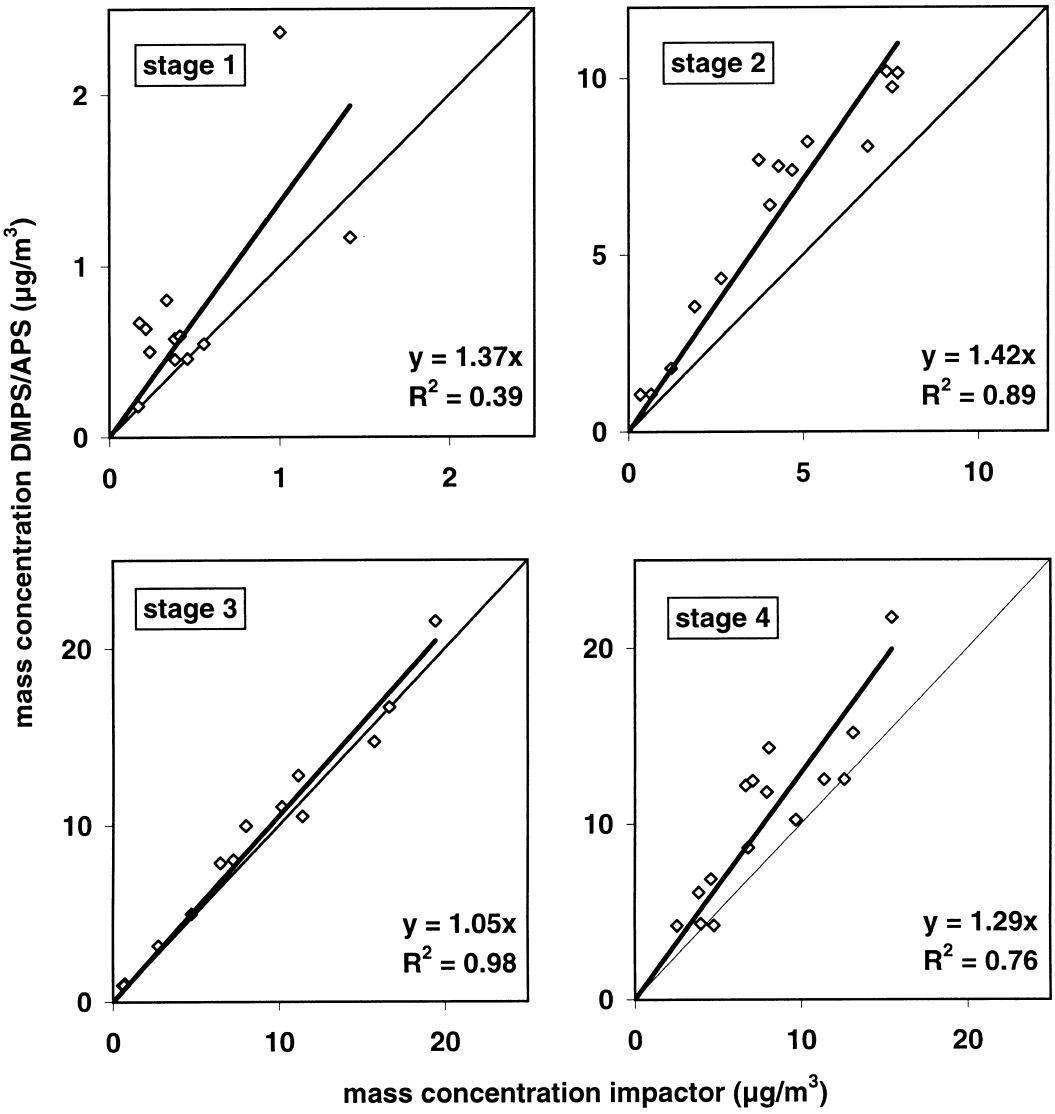

Fig. 4. Comparison of gravimetric mass (impactor) versus DMPS/APS for single impactor stages (scenario 1, 60% RH).

size-resolving DMPS/APS are obvious in the impactor-derived mass concentration, for different air masses resulting in different modes and concentrations. The gravimetrically mass distributions seem to be shifted to larger particles. This trend is quantified for all 15 samples for the total mass concentration (<3.5 µm D_{ae}) shown in Fig. 3 and for the size segregated data in Fig. 4. A good correlation is found both for the total mass and for every individual impactor stage except for the smallest particles. The mass concentration calculated from the number distribution is systematically higher, than the gravimetric mass of the impactor samples by 23% and 9% for scenarios 1 and 2, respectively (slope = 1.23 and 1.09, Fig. 3). The sensitivity of these results to hygroscopic growth factor and density used in the 2 scenarios is obvious.

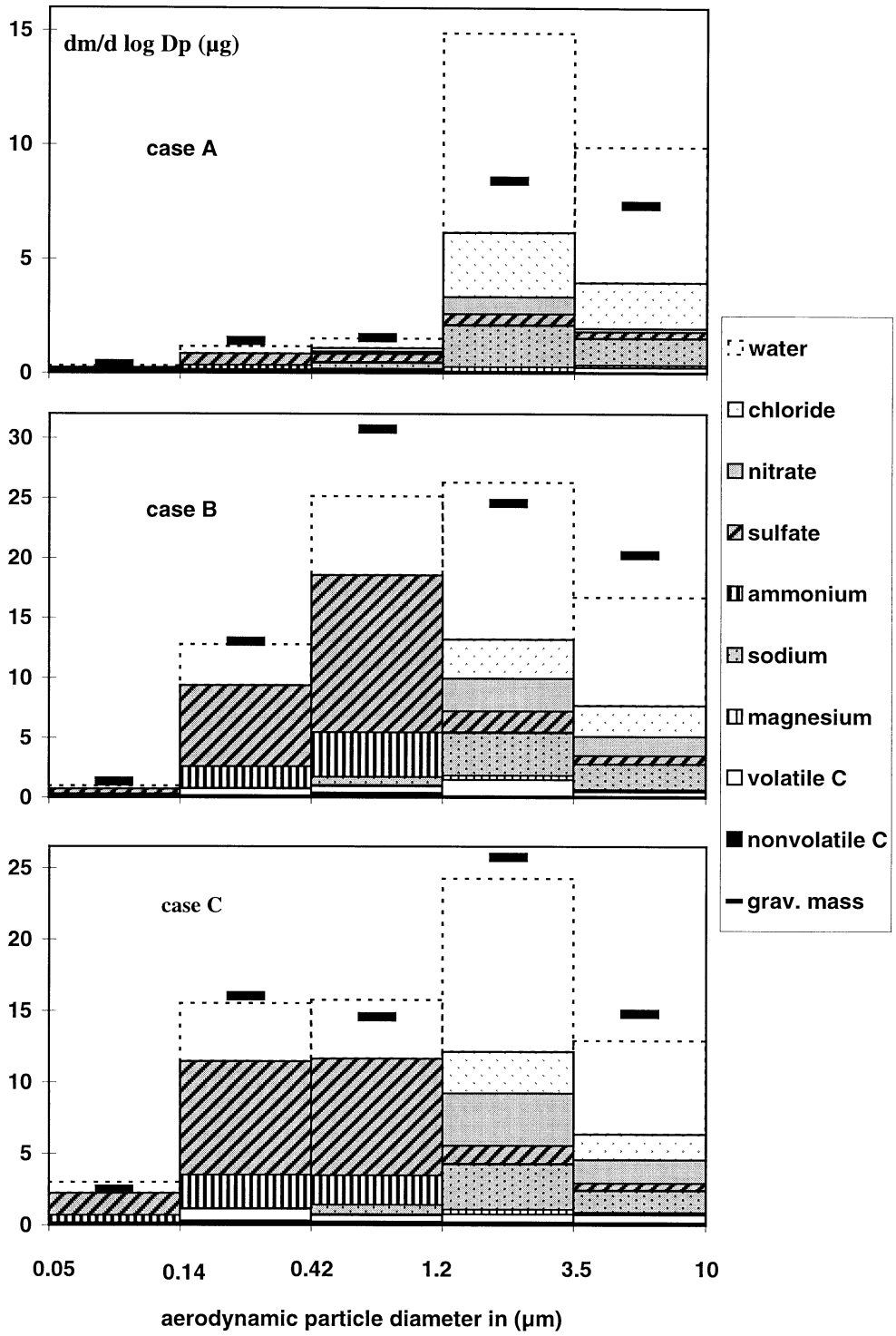

Fig. 5. Mass size distributions (60% RH) derived from chemical analysis (bar) and gravimetric mass (dash).

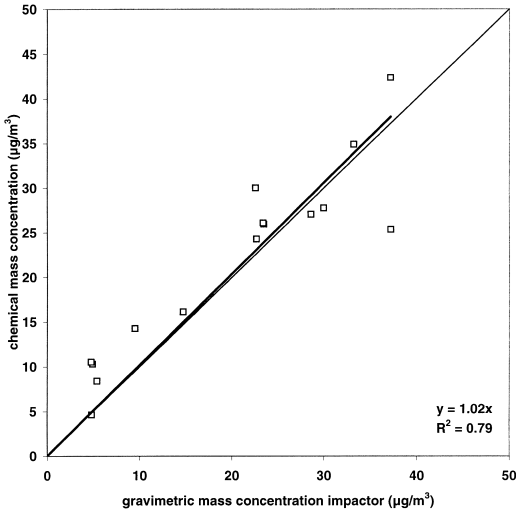

Fig. 6. Comparison of gravimetric versus chemical mass concentration (sum over 4 impactor stages, Stokes diameter <3 µm)

For the individual impactor stages, however, differences are much larger. Fig. 4 shows the size segregated correlation of mass concentration calculated with scenario 1 (scenario 2 lead to comparable results, but generally lower slope of the regression). The regression for smallest particles (0.05–0.14 µm D_{ae}) has a low coefficient of determination ($R^2 = 0.39$), which is mainly due to larger relative errors in the gravimetric analysis since absolute masses were <76 µg. The reason that the masses derived from DMPS/APS measurements for impactor stage 2 (0.14–0.42 µm D_{ae}) are in general much higher than for the gravimetric determination while masses for stage 3 (0.42–1.2 µm D_{ae}) show much better agreement is not clear. The reason might be a systematic error in sizing as discussed above. Generally, these trends are independent of the level of pollution (mass concentration and chemical composition). The difference for particles in the coarse mode is very likely due to an over-determination of the number of particles by the APS.

Since the calculated overall uncertainties are larger than the difference in the total mass concentrations derived from the different approaches, we conclude that these uncertainties are in fact valid uncertainties for the size dependent mass concentration. However, the number distribution-derived mass is mostly higher than the chemically and gravimetrically determined mass. This can be explained by sampling losses of the impactor. Wang and John (1988) determined a sampling loss for a Berner impactor for ammonium sulphate of 10% at 60% RH. Since ammonium sulphate was the main compound in the submicrometer size range during ACE-2, this value can be assigned to our approach. Applied to scenario 2, there remains no systematic difference.

4.2. Chemical mass balance

Chemical mass balance for the 3 cases is presented in Fig. 5. In polluted cases B and C, particles smaller 1.2 µm in diameter contain mostly sulphate, ammonium and small amounts of carbon. Particles in the coarse mode contain mainly sea-salt, where chloride has been partly replaced by nitrate and to some extend by sulphate. Water was calculated as described above. Generally, the agreement is good, a quantitative comparison is presented in Figs. 6 and 7. A regression of chemical mass concentration on gravimetric mass concentration results in a slope of 1.02 and a coefficient of determination, R^2, of 0.79. The uncertainties for the determination of both the gravimetric mass concentration and the chemical mass concentration are in the range of $\pm 20\%$ and are larger than the differences between the gravimetric and chemical results. This result is valid for particle size intervals corresponding to the impactor stages 2 to 4 as well as for the integral over particle size. Nevertheless, the uncertainty for smallest particles is unacceptably large. In addition, the over-determination of the chemical compounds for large particles (stage 4) has to be addressed. Insoluble material estimated from element analysis (PIXE-analysis, particle induced X-ray emission) from filter samples performed at the University of Lund, Sweden, accounts for less than 3% of the total mass. This amount is expected to be mostly in the coarse mode range, which increases the chemical mass concentration further, but might explain the difference in mass balance within the coarse mode although the ionic composition is only slightly different (Table 2). The main error is expected to be in the water amount. Its calculation for the coarse mode is based on the ionic composition of sea-salt assuming an additional growth for nitrate and chloride salts, which might not be the case. Furthermore, the

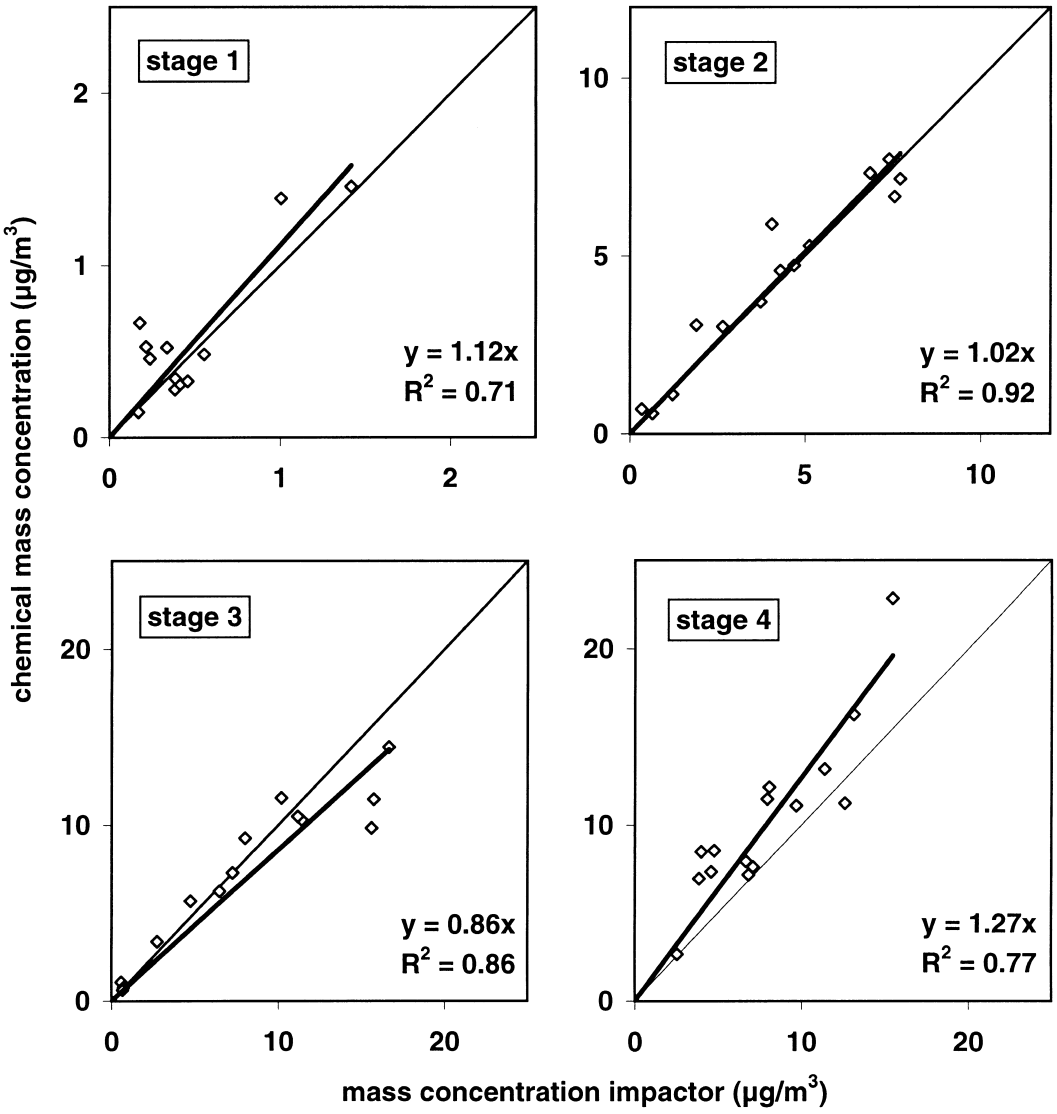

Fig. 7. Comparison of gravimetric versus chemical mass for single impactor stages.

abundance of insoluble (crustal) material or carbon, e.g., organic acids in this size range (Neusüß et al. A new analytical approach for size-resolved speciation of organic compounds in atmospheric aerosol particles: methods and first results. *Geophys. Res.* **2000**, in press) might lead to a reduction of water uptake. For all particle sizes the amount of water is a critical value since it is difficult to determine for bulk samples of atmospheric particles. The application of the growth factors determined by a HTDMA for individual, suspended particles to the water amount of bulk samples is highly uncertain.

Putaud et al. (2000) performed a closure study for the aerosol on the Canary Islands during ACE-2. They compared the total submicrometer chemical volume with the particle volume derived from number size distributions (as integral over the corresponding size range). A comparison of their results with ours would be useful but is

difficult. They used filters instead of impactors leading to different sampling performances (positive and negative sampling artefacts, different size ranges). The different methods for the specification of carbon is expected to provide similar total carbon values but different classification concerning organic and elemental carbon. The analysis of the ions is expected to be comparable, which is demonstrated by the successful intercomparison. Therefore, the uncertainties estimated by Putaud et al. are similar for ionic concentrations, but larger for carbon determination and sampling.

For comparison of the chemical composition of different air masses see Quinn et al. (2000).

5. Conclusions

A 3-way comparison of mass concentrations derived from gravimetric analysis and chemical analysis of impactor samples, and from number size distributions was conducted on concurrently collected samples. The mass concentrations agree within the uncertainties of the methods depending on the size of the particles, but are independent of the degree of pollution. The agreement within about 20% is surprisingly good considering the large differences in size and shape of the particles (assuming only spherical particles) and the totally different methods of characterisation. Uncertainties in the mass concentration of about 20% lead to uncertainties of the scattering of the particles in the same range (Waggoner and Weiss, 1980. Whether these values are acceptably small or not cannot concluded here.

Total mass concentrations ($D_p < 3$ μm Stokes diameter) derived from DMPS/APS-number-size distributions are higher than mass concentrations determined gravimetrically from impactor samples. Sampling losses might explain (partly) the differences as well as uncertainties of the measurements. The overall errors for each of the methods are in the range of $\pm 20\%$. Higher number-derived mass concentrations are mainly observed for small particles (37% for 0.05–0.14 μm, and 42% for 0.14–0.42 μm D_{ae}) and coarse mode particles (29% for 1.2–3.5 μm D_{ae}). Accumulation mode particles (0.42–1.2 μm D_{ae}) show the best agreement with a difference of only 5%. These effects can be due to sizing errors of one or both methods. Precise absolute calibrations of impactors and DMPS/APS-systems are required to reduce these uncertainties.

The chemical mass balance (chemical versus gravimetric mass) for the sum of the impactor stages 1 to 4 (0.05–3.5 μm D_{ae}) is very good, with a difference of 2%, in spite of obvious differences between single impactor stages. Thus, agreement (2% difference) is best for particles between 0.14 and 0.42 μm diameter. This fact can be attributed to (i) the measured humidity growth (compared to the estimated growth for coarse mode particles), (ii) the simple chemical composition (compared to all larger particle size fractions), and (iii) the higher mass loading of the impactor (compared to smaller particles). But even for other size classes the agreement (with differences between 12 and 27%) is within the measurement uncertainties of about $\pm 20\%$ for both, gravimetric and the chemical analysis.

The determination of the water content within particles is critical for the chemical mass balance as well as for the connection between dry number-size distribution and gravimetric mass determined at higher humidity. To improve the results of the chemical mass balance precise measurements of water, especially of large particles, need to be performed. Comparison of single particle growth factors with bulk amount of water are needed. The density of particles is difficult to measure, requiring instead an assumption based on chemical composition. In addition, the characteristics of the sampling inlet and the sampling performance of the impactor have to be determined. A better APS might minimise false counts and might therefore provide a better chance of a successful 3-way mass closure in the supermicrometer size range. Number size distribution measurements at a relative humidity comparable to the impactor sampling RH would reduce the uncertainty concerning a shape correction of the particles.

It seems to be possible to assign a chemical composition measured with an impactor with only a few stages to aerosol modes determined with the better size resolving number distributions, without applying a questionable inversion algorithm to impactor measurements.

6. Acknowledgements

The contributions of A. Thomas, B. Gerlach and S. Philippin during the field campaign is

gratefully acknowledged. We thank E. Swietlicki for the possibility to perform PIXE analysis in Lund, Sweden. This research was conducted as part of the second Aerosol Characterisation Experiment (ACE-2), which is a contribution to the International Global Atmospheric Chemistry (IGAC) core project of the International Geosphere-Biosphere Programme (IGBP). Financial support for the measurements and analyses was provided by the DGXII of the European Commission (contracts Nr. ENV4-CZ95-0032 and Nr. ENV4-CT95-0108) and by the Institute for Tropospheric Research, Leipzig. This is University of Washington, JISAO contribution 650.

REFERENCES

Beck, W. and Engelhardt, H. 1992. Capillary electrophoresis of organic and inorganic cations with indirect UV detection. *Chromatographia* **33**, 313–316.

Berner, A. and Lürzer, C. 1980. Mass size distributions of traffic aerosols at Vienna. *J. Phys. Chem.* **84**, 2079–2083.

Birmili, W., Stratmann, F. and Wiedensohler, A. 1999. Design of a DMA-based size spectrometer for a large particle size range and stable operation. *J. Aerosol Sci.* **30**, 549–553.

Charlson, R. J., Langner, J., Rodhe, H., Leovy, C. B. and Warren, S. G. 1991. Perturbation of the northern hemisphere radiative balance by backscattering of anthropogenic sulfate aerosols. *Tellus* **43A/B**, 152–163.

Hillamo, R. E. and Kauppinen, E. I. 1991. On the performance of the Berner low pressure impactor. *Aer. Sci. Technol.* **14**, 33–47.

Howell, S., Pszenny, A. A. P., Quinn, P. and Huebert, B. 1998. A field intercomparison of three cascade impactors. *Aer. Sci. Technol.* **29**, 475–492.

Petzold, A. 1995. *Messung von Rußimmissionen: Der Photoakustische Rußsensor zur in-situ Detektion und eine thermische Methode zur Analyse von Filterproben.* Thesis. Technical University Munich, Germany.

Putaud, J.-P. and co-authors. 2000. Chemical mass closure and origin assessment of the submicron aerosol in the marine boundary layer and the free troposphere at Tenerife during ACE-2. *Tellus* **52B**, 141–168.

Quinn, P. K. and Coffman, D. J. 1998. Local closure during the first aerosol characterization experiment (ACE1): aerosol mass concentration and scattering and backscattering coefficients. *J. Geophys. Res.* **103**, 16,575–16,596.

Quinn, P. K., Anderson, T. L., Bates, T. S., Dlugi, R., Heintzenberg, J., Hoyningen-Huene von, W., Kulmala, M., Russell, P. B. and Swietlicki, E. 1996. Closure in tropospheric aerosol-climate research: a review and future needs for addressing aerosol direct shortwave radiative forcing. *Contr. Atmos. Phys.* **69**, 547–577.

Quinn, P. K., Bates, T. S., Coffman, D. J., Miller, J. E., Covert, D. S., Putand, J. P. and Neusüß, C. 2000. A comparison of aerosol chemical and optical properties from the first and second Aerosol Characterization Experiment. *Tellus* **52B**, 239–257.

Reineking, A., Scheibel, H. G., Hussin, A., Becker, K. H. and Porstendörfer, J. 1984. Measurements of stage efficiency functions including interstage losses for a Sierra and Berner impactor and evaluation of data by a modified simplex method. *J. Aerosol Sci.* **15**, 376–380.

Röder, A. and Bächmann, K. 1995. Simultaneous determination of organic and inorganic anions in the sub-µmol/l range in rain water by capillary zone electrophoresis. *J. Chromatogr.* **A689**, 305–311.

Russell, P. and Heintzenberg, J. 2000. An overview of the ACE-2 clear sky column closure experiment (CLEARCOLUMN). *Tellus* **52B**, 463–483.

Swietlicki, E., Zhou, J., Covert, D. S., Hämeri, K., Busch, B., Väkeva, M., Dusek, U., Berg, O. H., Wiedensohler, A., Aalto, P., Mäkelä, J., Papaspiropoulos, G., Mentes, B., Frank, G. and Stratmann, F. 2000. Hygroscopic properties of aerosol particles in the north-eastern Atlantic during ACE-2. *Tellus* **52B**, 201–227.

Tang, I. N. and Munkelwitz, H. R. 1994. Water activities, densities, and refractive indices of aqueous sulfates and sodium nitrate droplets of atmospheric importance. *J. Geophys. Res.* **99**, 18,801–18,808.

Tang, I. N., Tridico, A. C. and Fung, K. H. 1997. Thermodynamic and optical properties of sea salt aerosols. *J. Geophys. Res.* **102**, 23,269–23,275.

Twomey, S. 1977. The influence of pollution on the shortwave albedo of clouds. *J. Atmos. Sci.* **34**, 1149–1152.

Waggoner, A. P. and Weiss, R. E. 1980. Comparison of fine particle mass concentration and light scattering extinction in ambient aerosols. *Atmos. Environ.* **14**, 623–626.

Wang, H.-C. and John, W. 1988. Characteristics of the Berner impactor for sampling inorganic ions. *Aer. Sci. Technol.* **8**, 157–172.

Yang, Q., Smeyers-Verbecke, J., Wu, W., Kots, M. S. and Massart, D. L. 1994. Simultaneous separation of ammonium an alkali, alkaline earth and transition metal ions in aqueous-organic media capillary ion analysis. *J. Chromatogr.* **A688**, 339–349.